

Measurement of the Effective Weak Mixing Angle in $p\bar{p} \rightarrow Z/\gamma^* \rightarrow \ell^+ \ell^-$ Events

V. M. Abazov,³¹ B. Abbott,⁶⁷ B. S. Acharya,²⁵ M. Adams,⁴⁶ T. Adams,⁴⁴ J. P. Agnew,⁴¹ G. D. Alexeev,³¹ G. Alkhazov,³⁵ A. Alton,^{56,a} A. Askew,⁴⁴ S. Atkins,⁵⁴ K. Augsten,⁷ V. Aushev,³⁸ Y. Aushev,³⁸ C. Avila,⁵ F. Badaud,¹⁰ L. Bagby,⁴⁵ B. Baldin,⁴⁵ D. V. Bandurin,⁷⁴ S. Banerjee,²⁵ E. Barberis,⁵⁵ P. Baringer,⁵³ J. F. Bartlett,⁴⁵ U. Bassler,¹⁵ V. Bazterra,⁴⁶ A. Bean,⁵³ M. Begalli,² L. Bellantoni,⁴⁵ S. B. Beri,²³ G. Bernardi,¹⁴ R. Bernhard,¹⁹ I. Bertram,³⁹ M. Besançon,¹⁵ R. Beuselinck,⁴⁰ P. C. Bhat,⁴⁵ S. Bhatia,⁵⁸ V. Bhatnagar,²³ G. Blazey,⁴⁷ S. Blessing,⁴⁴ K. Bloom,⁵⁹ A. Boehnlein,⁴⁵ D. Boline,⁶⁴ E. E. Boos,³³ G. Borissov,³⁹ M. Borysova,^{38,b} A. Brandt,⁷¹ O. Brandt,²⁰ M. Brochmann,⁷⁵ R. Brock,⁵⁷ A. Bross,⁴⁵ D. Brown,¹⁴ X. B. Bu,⁴⁵ M. Buehler,⁴⁵ V. Buescher,²¹ V. Bunichev,³³ S. Burdin,^{39,c} C. P. Buszello,³⁷ E. Camacho-Pérez,²⁸ B. C. K. Casey,⁴⁵ H. Castilla-Valdez,²⁸ S. Caughron,⁵⁷ S. Chakrabarti,⁶⁴ K. M. Chan,⁵¹ A. Chandra,⁷³ E. Chapon,¹⁵ G. Chen,⁵³ S. W. Cho,²⁷ S. Choi,²⁷ B. Choudhary,²⁴ S. Cihangir,^{45,*} D. Claes,⁵⁹ J. Clutter,⁵³ M. Cooke,^{45,d} W. E. Cooper,⁴⁵ M. Corcoran,^{73,*} F. Couderc,¹⁵ M.-C. Cousinou,¹² J. Cuth,²¹ D. Cutts,⁷⁰ A. Das,⁷² G. Davies,⁴⁰ S. J. de Jong,^{29,30} E. De La Cruz-Burelo,²⁸ F. Déliot,¹⁵ R. Demina,⁶³ D. Denisov,⁴⁵ S. P. Denisov,³⁴ S. Desai,⁴⁵ C. Deterre,^{41,e} K. DeVaughan,⁵⁹ H. T. Diehl,⁴⁵ M. Diesburg,⁴⁵ P. F. Ding,⁴¹ A. Dominguez,⁵⁹ A. Drutskoy,^{32,f} A. Dubey,²⁴ L. V. Dudko,³³ A. Duperrin,¹² S. Dutt,²³ M. Eads,⁴⁷ D. Edmunds,⁵⁷ J. Ellison,⁴³ V. D. Elvira,⁴⁵ Y. Enari,¹⁴ H. Evans,⁴⁹ A. Evdokimov,⁴⁶ V. N. Evdokimov,³⁴ A. Fauré,¹⁵ L. Feng,⁴⁷ T. Ferbel,⁶³ F. Fiedler,²¹ F. Filthaut,^{29,30} W. Fisher,⁵⁷ H. E. Fisk,⁴⁵ M. Fortner,⁴⁷ H. Fox,³⁹ J. Franc,⁷ S. Fuess,⁴⁵ P. H. Garbincius,⁴⁵ A. Garcia-Bellido,⁶³ J. A. García-González,²⁸ V. Gavrilov,³² W. Geng,^{12,57} C. E. Gerber,⁴⁶ Y. Gershtein,⁶⁰ G. Ginther,⁴⁵ O. Gogota,³⁸ G. Golovanov,³¹ P. D. Grannis,⁶⁴ S. Greder,¹⁶ H. Greenlee,⁴⁵ G. Grenier,¹⁷ Ph. Gris,¹⁰ J.-F. Grivaz,¹³ A. Grohsjean,^{15,e} S. Grünendahl,⁴⁵ M. W. Grünewald,²⁶ T. Guillemain,¹³ G. Gutierrez,⁴⁵ P. Gutierrez,⁶⁷ J. Haley,⁶⁸ L. Han,⁴ K. Harder,⁴¹ A. Harel,⁶³ J. M. Hauptman,⁵² J. Hays,⁴⁰ T. Head,⁴¹ T. Hebbeker,¹⁸ D. Hedin,⁴⁷ H. Hegab,⁶⁸ A. P. Heinson,⁴³ U. Heintz,⁷⁰ C. Hensel,¹ I. Heredia-De La Cruz,^{28,g} K. Herner,⁴⁵ G. Hesketh,^{41,h} M. D. Hildreth,⁵¹ R. Hirosky,⁷⁴ T. Hoang,⁴⁴ J. D. Hobbs,⁶⁴ B. Hoeneisen,⁹ J. Hogan,⁷³ M. Hohlfeld,²¹ J. L. Holzbauer,⁵⁸ I. Howley,⁷¹ Z. Hubacek,^{7,15} V. Hynek,⁷ I. Iashvili,⁶² Y. Ilchenko,⁷² R. Illingworth,⁴⁵ A. S. Ito,⁴⁵ S. Jabeen,^{45,i} M. Jaffré,¹³ A. Jayasinghe,⁶⁷ M. S. Jeong,²⁷ R. Jesik,⁴⁰ P. Jiang,^{4,*} K. Johns,⁴² E. Johnson,⁵⁷ M. Johnson,⁴⁵ A. Jonckheere,⁴⁵ P. Jonsson,⁴⁰ J. Joshi,⁴³ A. W. Jung,^{45,j} A. Juste,³⁶ E. Kajfasz,¹² D. Karmanov,³³ I. Katsanos,⁵⁹ M. Kaur,²³ R. Kehoe,⁷² S. Kermiche,¹² N. Khalatyan,⁴⁵ A. Khanov,⁶⁸ A. Kharchilava,⁶² Y. N. Kharzheev,³¹ I. Kiselevich,³² J. M. Kohli,²³ A. V. Kozelov,³⁴ J. Kraus,⁵⁸ A. Kumar,⁶² A. Kupco,⁸ T. Kurča,¹⁷ V. A. Kuzmin,³³ S. Lammers,⁴⁹ P. Lebrun,¹⁷ H. S. Lee,²⁷ S. W. Lee,⁵² W. M. Lee,^{45,*} X. Lei,⁴² J. Lellouch,¹⁴ D. Li,¹⁴ H. Li,⁷⁴ L. Li,⁴³ Q. Z. Li,⁴⁵ J. K. Lim,²⁷ D. Lincoln,⁴⁵ J. Linnemann,⁵⁷ V. V. Lipaev,^{34,*} R. Lipton,⁴⁵ H. Liu,⁷² Y. Liu,⁴ A. Lobodenko,³⁵ M. Lokajicek,⁸ R. Lopes de Sa,⁴⁵ R. Luna-Garcia,^{28,k} A. L. Lyon,⁴⁵ A. K. A. Maciel,¹ R. Madar,¹⁹ R. Magaña-Villalba,²⁸ S. Malik,⁵⁹ V. L. Malyshev,³¹ J. Mansour,²⁰ J. Martínez-Ortega,²⁸ R. McCarthy,⁶⁴ C. L. McGivern,⁴¹ M. M. Meijer,^{29,30} A. Melnitchouk,⁴⁵ D. Menezes,⁴⁷ P. G. Mercadante,³ M. Merkin,³³ A. Meyer,¹⁸ J. Meyer,^{20,l} F. Miconi,¹⁶ N. K. Mondal,²⁵ M. Mulhearn,⁷⁴ E. Nagy,¹² M. Narain,⁷⁰ R. Nayyar,⁴² H. A. Neal,⁵⁶ J. P. Negret,⁵ P. Neustroev,³⁵ H. T. Nguyen,⁷⁴ T. Nunnemann,²² J. Orduna,⁷⁰ N. Osman,¹² A. Pal,⁷¹ N. Parashar,⁵⁰ V. Parihar,⁷⁰ S. K. Park,²⁷ R. Partridge,^{70,m} N. Parua,⁴⁹ A. Patwa,^{65,n} B. Penning,⁴⁰ M. Perfilov,³³ Y. Peters,⁴¹ K. Petridis,⁴¹ G. Petrillo,⁶³ P. Pétroff,¹³ M.-A. Pleier,⁶⁵ V. M. Podstavkov,⁴⁵ A. V. Popov,³⁴ M. Prewitt,⁷³ D. Price,⁴¹ N. Prokopenko,³⁴ J. Qian,⁵⁶ A. Quadt,²⁰ B. Quinn,⁵⁸ P. N. Ratoff,³⁹ I. Razumov,³⁴ I. Ripp-Baudot,¹⁶ F. Rizatdinova,⁶⁸ M. Rominsky,⁴⁵ A. Ross,³⁹ C. Royon,⁸ P. Rubinov,⁴⁵ R. Ruchti,⁵¹ G. Sajot,¹¹ A. Sánchez-Hernández,²⁸ M. P. Sanders,²² A. S. Santos,^{1,o} G. Savage,⁴⁵ M. Savitskyi,³⁸ L. Sawyer,⁵⁴ T. Scanlon,⁴⁰ R. D. Schamberger,⁶⁴ Y. Scheglov,^{35,*} H. Schellman,^{69,48} M. Schott,²¹ C. Schwanenberger,⁴¹ R. Schwienhorst,⁵⁷ J. Sekaric,⁵³ H. Severini,⁶⁷ E. Shabalina,²⁰ V. Shary,¹⁵ S. Shaw,⁴¹ A. A. Shchukin,³⁴ O. Shkola,³⁸ V. Simak,⁷ P. Skubic,⁶⁷ P. Slattery,⁶³ G. R. Snow,⁵⁹ J. Snow,⁶⁶ S. Snyder,⁶⁵ S. Söldner-Rembold,⁴¹ L. Sonnenschein,¹⁸ K. Soustruznik,⁶ J. Stark,¹¹ N. Stefaniuk,³⁸ D. A. Stoyanova,³⁴ M. Strauss,⁶⁷ L. Suter,⁴¹ P. Svoisky,⁷⁴ M. Titov,¹⁵ V. V. Tokmenin,³¹ Y.-T. Tsai,⁶³ D. Tsybychev,⁶⁴ B. Tuchming,¹⁵ C. Tully,⁶¹ L. Uvarov,³⁵ S. Uvarov,³⁵ S. Uzunyan,⁴⁷ R. Van Kooten,⁴⁹ W. M. van Leeuwen,²⁹ N. Varelas,⁴⁶ E. W. Varnes,⁴² I. A. Vasilyev,³⁴ A. Y. Verkheev,³¹ L. S. Vertogradov,³¹ M. Verzocchi,⁴⁵ M. Vesterinen,⁴¹ D. Vilanova,¹⁵ P. Vokac,⁷ H. D. Wahl,⁴⁴ C. Wang,⁴ M. H. L. S. Wang,⁴⁵ J. Warchol,^{51,*} G. Watts,⁷⁵ M. Wayne,⁵¹ J. Weichert,²¹ L. Welty-Rieger,⁴⁸ M. R. J. Williams,^{49,p} G. W. Wilson,⁵³ M. Wobisch,⁵⁴ D. R. Wood,⁵⁵ T. R. Wyatt,⁴¹ Y. Xiang,⁴ Y. Xie,⁴⁵ R. Yamada,⁴⁵ S. Yang,⁴ T. Yasuda,⁴⁵ Y. A. Yatsunenkov,³¹

W. Ye,⁶⁴ Z. Ye,⁴⁵ H. Yin,⁴⁵ K. Yip,⁶⁵ S. W. Youn,⁴⁵ J. M. Yu,⁵⁶ J. Zennamo,⁶² T. G. Zhao,⁴¹ B. Zhou,⁵⁶ J. Zhu,⁵⁶
M. Zielinski,⁶³ D. Zieminska,⁴⁹ and L. Zivkovic^{14,q}

(The D0 Collaboration)

¹LAFEX, Centro Brasileiro de Pesquisas Físicas, Rio de Janeiro, Rio de Janeiro 22290, Brazil

²Universidade do Estado do Rio de Janeiro, Rio de Janeiro, Rio de Janeiro 20550, Brazil

³Universidade Federal do ABC, Santo André, São Paulo 09210, Brazil

⁴University of Science and Technology of China, Hefei 230026, People's Republic of China

⁵Universidad de los Andes, Bogotá 111711, Colombia

⁶Charles University, Faculty of Mathematics and Physics, Center for Particle Physics, 116 36 Prague 1, Czech Republic

⁷Czech Technical University in Prague, 116 36 Prague 6, Czech Republic

⁸Institute of Physics, Academy of Sciences of the Czech Republic, 182 21 Prague, Czech Republic

⁹Universidad San Francisco de Quito, Quito 170157, Ecuador

¹⁰LPC, Université Blaise Pascal, CNRS/IN2P3, Clermont, F-63178 Aubière Cedex, France

¹¹LPSC, Université Joseph Fourier Grenoble 1, CNRS/IN2P3, Institut National Polytechnique de Grenoble, F-38026 Grenoble Cedex, France

¹²CPPM, Aix-Marseille Université, CNRS/IN2P3, F-13288 Marseille Cedex 09, France

¹³LAL, Univ. Paris-Sud, CNRS/IN2P3, Université Paris-Saclay, F-91898 Orsay Cedex, France

¹⁴LPNHE, Universités Paris VI and VII, CNRS/IN2P3, F-75005 Paris, France

¹⁵CEA Saclay, Irfu, SPP, F-91191 Gif-Sur-Yvette Cedex, France

¹⁶IPHC, Université de Strasbourg, CNRS/IN2P3, F-67037 Strasbourg, France

¹⁷IPNL, Université Lyon 1, CNRS/IN2P3, F-69622 Villeurbanne Cedex, France and Université de Lyon, F-69361 Lyon CEDEX 07, France

¹⁸III. Physikalisches Institut A, RWTH Aachen University, 52056 Aachen, Germany

¹⁹Physikalisches Institut, Universität Freiburg, 79085 Freiburg, Germany

²⁰II. Physikalisches Institut, Georg-August-Universität Göttingen, 37073 Göttingen, Germany

²¹Institut für Physik, Universität Mainz, 55099 Mainz, Germany

²²Ludwig-Maximilians-Universität München, 80539 München, Germany

²³Panjab University, Chandigarh 160014, India

²⁴Delhi University, Delhi-110 007, India

²⁵Tata Institute of Fundamental Research, Mumbai-400 005, India

²⁶University College Dublin, Dublin 4, Ireland

²⁷Korea Detector Laboratory, Korea University, Seoul 02841, Korea

²⁸CINVESTAV, Mexico City 07360, Mexico

²⁹Nikhef, Science Park, 1098 XG Amsterdam, Netherlands

³⁰Radboud University Nijmegen, 6525 AJ Nijmegen, Netherlands

³¹Joint Institute for Nuclear Research, Dubna 141980, Russia

³²Institute for Theoretical and Experimental Physics, Moscow 117259, Russia

³³Moscow State University, Moscow 119991, Russia

³⁴Institute for High Energy Physics, Protvino, Moscow region 142281, Russia

³⁵Petersburg Nuclear Physics Institute, St. Petersburg 188300, Russia

³⁶Institució Catalana de Recerca i Estudis Avançats (ICREA) and Institut de Física d'Altes Energies (IFAE), 08193 Bellaterra (Barcelona), Spain

³⁷Uppsala University, 751 05 Uppsala, Sweden

³⁸Taras Shevchenko National University of Kyiv, Kiev 01601, Ukraine

³⁹Lancaster University, Lancaster LA1 4YB, United Kingdom

⁴⁰Imperial College London, London SW7 2AZ, United Kingdom

⁴¹The University of Manchester, Manchester M13 9PL, United Kingdom

⁴²University of Arizona, Tucson, Arizona 85721, USA

⁴³University of California Riverside, Riverside, California 92521, USA

⁴⁴Florida State University, Tallahassee, Florida 32306, USA

⁴⁵Fermi National Accelerator Laboratory, Batavia, Illinois 60510, USA

⁴⁶University of Illinois at Chicago, Chicago, Illinois 60607, USA

⁴⁷Northern Illinois University, DeKalb, Illinois 60115, USA

⁴⁸Northwestern University, Evanston, Illinois 60208, USA

⁴⁹Indiana University, Bloomington, Indiana 47405, USA

⁵⁰Purdue University Calumet, Hammond, Indiana 46323, USA

⁵¹University of Notre Dame, Notre Dame, Indiana 46556, USA

- ⁵²Iowa State University, Ames, Iowa 50011, USA
⁵³University of Kansas, Lawrence, Kansas 66045, USA
⁵⁴Louisiana Tech University, Ruston, Louisiana 71272, USA
⁵⁵Northeastern University, Boston, Massachusetts 02115, USA
⁵⁶University of Michigan, Ann Arbor, Michigan 48109, USA
⁵⁷Michigan State University, East Lansing, Michigan 48824, USA
⁵⁸University of Mississippi, University, Mississippi 38677, USA
⁵⁹University of Nebraska, Lincoln, Nebraska 68588, USA
⁶⁰Rutgers University, Piscataway, New Jersey 08855, USA
⁶¹Princeton University, Princeton, New Jersey 08544, USA
⁶²State University of New York, Buffalo, New York 14260, USA
⁶³University of Rochester, Rochester, New York 14627, USA
⁶⁴State University of New York, Stony Brook, New York 11794, USA
⁶⁵Brookhaven National Laboratory, Upton, New York 11973, USA
⁶⁶Langston University, Langston, Oklahoma 73050, USA
⁶⁷University of Oklahoma, Norman, Oklahoma 73019, USA
⁶⁸Oklahoma State University, Stillwater, Oklahoma 74078, USA
⁶⁹Oregon State University, Corvallis, Oregon 97331, USA
⁷⁰Brown University, Providence, Rhode Island 02912, USA
⁷¹University of Texas, Arlington, Texas 76019, USA
⁷²Southern Methodist University, Dallas, Texas 75275, USA
⁷³Rice University, Houston, Texas 77005, USA
⁷⁴University of Virginia, Charlottesville, Virginia 22904, USA
⁷⁵University of Washington, Seattle, Washington 98195, USA



(Received 12 October 2017; published 13 June 2018)

We present a measurement of the effective weak mixing angle parameter $\sin^2\theta_{\text{eff}}^f$ in $p\bar{p} \rightarrow Z/\gamma^* \rightarrow \mu^+\mu^-$ events at a center-of-mass energy of 1.96 TeV, collected by the D0 detector at the Fermilab Tevatron Collider and corresponding to 8.6 fb^{-1} of integrated luminosity. The measured value of $\sin^2\theta_{\text{eff}}^f[\mu\mu] = 0.23016 \pm 0.00064$ is further combined with the result from the D0 measurement in $p\bar{p} \rightarrow Z/\gamma^* \rightarrow e^+e^-$ events, resulting in $\sin^2\theta_{\text{eff}}^f[\text{comb}] = 0.23095 \pm 0.00040$. This combined result is the most precise measurement from a single experiment at a hadron collider and is the most precise determination using the coupling of the Z/γ^* to light quarks.

DOI: [10.1103/PhysRevLett.120.241802](https://doi.org/10.1103/PhysRevLett.120.241802)

The weak mixing angle θ_W is a fundamental parameter of the standard model (SM). It governs the mechanism of spontaneous symmetry breaking of $SU(2) \times U(1)$ in which the original vector boson fields W and B_0 are transformed to the physical W^\pm , Z , and γ states. At tree level and in all orders of the on-shell renormalization scheme, the weak mixing angle also relates the W and Z boson masses by $\sin^2\theta_W = 1 - M_W^2/M_Z^2$. To include higher-order electroweak radiative corrections and allow comparison with experimental measurements, the effective weak mixing angle can be defined [1] in terms of the relative strengths of the axial vector and vector couplings, g_A^f and g_V^f , of the Z boson to fermions, f :

$$\sin^2\theta_{\text{eff}}^f = \frac{1}{4|Q_f|} \left(1 - \frac{g_V^f}{g_A^f} \right), \quad (1)$$

where Q_f is the electric charge of the fermions.

It is customary to quote the charged-lepton effective weak mixing angle parameter $\sin^2\theta_{\text{eff}}^e$, determined by measurements of observables around the Z -boson mass pole (M_Z). The effective mixing angle was precisely measured by the LEP Collaborations and the SLD Collaboration in different physics processes. The combined LEP and SLD result [1] gives a value of $\sin^2\theta_{\text{eff}}^e = 0.23153 \pm 0.00016$ at the energy scale $\mu = M_Z$. The two most precise individual measurements are from the measurement of b -quark forward-backward asymmetry at LEP ($\sin^2\theta_{\text{eff}}^e = 0.23221 \pm 0.00029$) and the measurement of the left-right polarization asymmetry at SLD ($\sin^2\theta_{\text{eff}}^e = 0.23098 \pm 0.00026$). An independent determination of the effective weak mixing angle at hadron colliders that is based on different combinations of fermions in the initial and final state from those in the e^+e^-

Published by the American Physical Society under the terms of the [Creative Commons Attribution 4.0 International](https://creativecommons.org/licenses/by/4.0/) license. Further distribution of this work must maintain attribution to the author(s) and the published article's title, journal citation, and DOI. Funded by SCOAP³.

measurements allows a precise test for new non-SM physics in the electroweak sector.

At the Tevatron, the weak mixing angle can be measured in the Drell-Yan process $p\bar{p} \rightarrow Z/\gamma^* \rightarrow \ell^+\ell^-$ through a forward-backward charge asymmetry, A_{FB} , defined by $A_{FB} = (N_F - N_B)/(N_F + N_B)$, where N_F and N_B are the numbers of forward and backward events. Forward (F) or backward (B) events are defined as those for which $\cos \theta^* > 0$ or $\cos \theta^* < 0$, where θ^* is the angle between the negatively charged lepton direction and the incoming proton direction in the Collins-Soper frame [2].

For the Z -to-fermion couplings, both $g_A^f = I_3^f$ and $g_V^f = I_3^f - 2Q_f \sin^2 \theta_W$ exist, whereas for the photon-to-fermion couplings there is only a vector coupling. I_3^f is the third component of the weak isospin of the fermion. The parity violation implicit in the forward-backward asymmetry arises from the interference between the vector and axial vector couplings. As the main subprocess for Drell-Yan production is the quark-antiquark annihilation $q\bar{q} \rightarrow \ell^+\ell^-$, A_{FB} depends upon both the couplings to light quarks and the couplings to leptons. The asymmetry can be measured as a function of the invariant mass of the dilepton pair. Since only the vector coupling of the Z boson depends on $\sin^2 \theta_W$, the information on $\sin^2 \theta_W$ comes from the asymmetry in the vicinity of the Z -boson pole. Away from the Z -boson mass pole, the asymmetry results from the interference of the axial vector Z coupling and vector photon coupling and depends upon the parton distribution functions (PDFs).

Measurements of $\sin^2 \theta_{\text{eff}}^{\ell}$ corresponding to the full data set at the Fermilab Tevatron Collider were performed by the CDF Collaboration using the $Z/\gamma^* \rightarrow \mu^+\mu^-$ channel [3] and the $Z/\gamma^* \rightarrow e^+e^-$ channel [4], and by the D0 Collaboration in the $Z/\gamma^* \rightarrow e^+e^-$ channel [5]. The weak mixing angle was also measured at the Large Hadron Collider (LHC) by the ATLAS, CMS, and LHCb Collaborations [6–8]. Because the directions of the initial quarks and antiquarks in the dominant subprocess $q\bar{q} \rightarrow Z/\gamma^* \rightarrow \ell^+\ell^-$ are unknown and have to be estimated in pp collisions, the precision of the LHC results is not as good as that of the Tevatron even with higher statistics.

This Letter reports a measurement of the effective weak mixing angle from the A_{FB} distribution as a function of the dimuon invariant mass using 8.6 fb^{-1} of data collected by the D0 detector at the Fermilab Tevatron Collider using the $Z/\gamma^* \rightarrow \mu^+\mu^-$ channel. The $Z/\gamma^* \rightarrow \mu^+\mu^-$ measurement is then combined with the D0 $Z/\gamma^* \rightarrow e^+e^-$ measurement [5].

The D0 detector comprises a central tracking system, a calorimeter, and a muon system [9–11]. The central tracking system consists of a silicon microstrip tracker and a scintillating fiber tracker, both located within a 1.9 T superconducting solenoidal magnet and optimized for tracking and vertexing capabilities for detector pseudorapidities of $|\eta_{\text{det}}| < 3$ [12]. Outside the solenoid, three

liquid-argon and uranium calorimeters provide coverage for $|\eta_{\text{det}}| < 3.5$ for electrons. The muon system is located outside of the calorimeters, providing coverage for $|\eta_{\text{det}}| < 2.0$. It consists of drift chambers and scintillators and 1.8 T iron toroidal magnets. The solenoid and toroid polarities are reversed every two weeks on average to reduce detector-induced asymmetries. Muons are identified using information from both the tracking system and the muon system. Muon momenta are measured using the tracking system information.

To maximize the event sample, data collected with all triggers are used in this analysis. Events are required to have at least two muon candidates reconstructed in the tracking system and the muon system. Both muon candidates [13] are required to have transverse momentum $p_T > 15 \text{ GeV}/c$ and $|\eta| < 1.8$ with at least one muon within $|\eta| < 1.6$. The two muon candidates must be isolated from jets in the event by requiring the sum of transverse momenta of tracks in the tracking system or transverse energy in the calorimeter within cones surrounding the muon candidate to be small. Muons must have a track in the tracking system matched with one in the muon system. To suppress backgrounds, the two matched tracks are required to point to the same $p\bar{p}$ interaction vertex and to have opposite charges. Events with muons nearly back to back are removed to reduce the cosmic ray background. Events are further required to have a reconstructed dimuon invariant mass $74 < M_{\mu\mu} < 110 \text{ GeV}/c^2$. The number of events satisfying these requirements is 481 239.

The Monte Carlo (MC) Drell-Yan $Z/\gamma^* \rightarrow \mu^+\mu^-$ sample is generated using leading-order PYTHIA [14] with the NNPDF3.0 [15] PDFs, followed by a GEANT-based simulation [16] of the D0 detector. Events from randomly selected beam crossings with the same instantaneous luminosity profile as data are overlaid on the simulated events to model detector noise and contributions from the presence of additional $p\bar{p}$ interactions. The PYTHIA MC samples are used to study the detector's geometric acceptance and the momentum scale and resolution of muons. Separate MC samples are generated for the four different polarity combinations of the solenoid and toroid magnetic fields.

The effective weak mixing angle, which is extracted from A_{FB} as a function of $M_{\mu\mu}$, depends strongly on the dimuon mass calibration. Therefore, it is critical to have a precise muon momentum measurement and a consistent measured mean value of $M_{\mu\mu}$ for all η , and each muon charge sign q and solenoid polarity S . The D0 muon momentum calibration and resolution smearing procedure [13] is applied to the MC simulation, so as to give agreement of the overall width and peak value of the $M_{\mu\mu}$ distribution with data. However, the muon momentum measurement, especially the scale of the reconstructed muon momentum, still depends on the charge and η of the muons due to imperfect alignment of the detector [17]. Such dependence would translate into a large systematic

uncertainty on the A_{FB} measurement. To reduce this dependence, an additional correction to the muon momentum, $\alpha(q, \eta, S)$, is applied to the data and MC separately. This factor is determined by requiring the mean of the $M_{\mu\mu}$ distribution over the full mass range in each (q, η, S) region to be consistent with the corresponding nominal value obtained from a generator-level MC sample after applying the same kinematic and acceptance cuts as those applied to the data. After the calibration, the mean values of $M_{\mu\mu}$ in data and MC samples are consistent to within statistical fluctuations. The additional calibration, together with the D0 muon calibration and resolution smearing procedure [13], reduces not only the q - η - S dependence, but also the potential effect from an imperfect modeling on the final-state radiation in the PYTHIA generator. The residual difference between data and MC $M_{\mu\mu}$ mean values is propagated to the uncertainty of the weak mixing angle measurement.

Additional corrections and reweightings are applied to the MC simulation to improve the agreement with data. The ratio between the MC and data efficiencies for the muon identification is measured using the tag-and-probe method [13] and applied to the MC distributions as a function of muon η . The simulation is further corrected for higher-order effects not included in PYTHIA by reweighting the MC events at the generator level in two dimensions (p_T and rapidity y of the Z boson) to match RESBOS [18] predictions. In addition, next-to-next-to-leading-order QCD corrections are applied as a function of Z -boson mass [18,19].

The sign of the track matched to the muon is used to determine the charge of the muon and to classify the event as forward or backward. The charge misidentification rate measured in the data is smaller than 0.4%. Since the opposite charge sign requirement is applied in the event selection, the probability of both muons charges being misidentified, thus transforming a forward event into a backward event or vice versa, is negligibly small.

Background is suppressed by the strict requirements on the muon tracks. The main remaining contribution is from multijet events, in which jets are misidentified as muons, which is estimated from data by selecting events with reversed muon isolation cuts in order to study the shape of the mass distribution of multijet events. The normalization of the multijet background is assumed to be same as that of the selected same-sign events after correcting for the presence of the misidentified signal events and the additional background contributions described below. The W + jets background is generated using ALPGEN [20] interfaced to PYTHIA for showering and hadronization. The $Z/\gamma^* \rightarrow \tau\tau$, diboson, and $t\bar{t}$ backgrounds are estimated using PYTHIA. In the dimuon mass range used for the effective weak mixing angle measurement, the multijet background is $0.68\% \pm 0.68\%$. A 100% uncertainty is used to safely cover the bias due to corrections for the misidentified signal events. The sum of the W + jets,

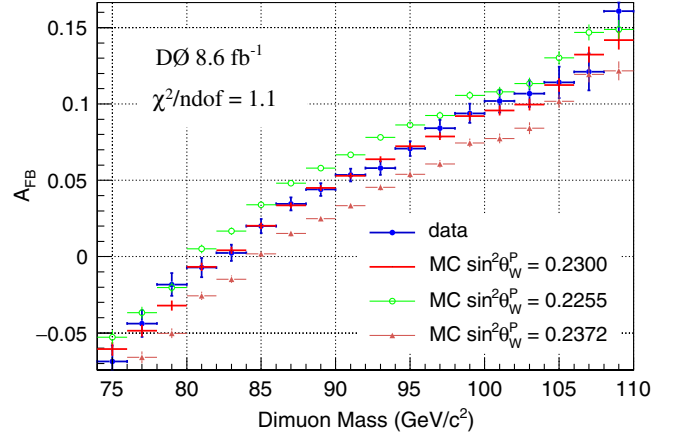


FIG. 1. Comparison between the A_{FB} distributions in the background-subtracted data and the MC with different $\sin^2 \theta_W^p$ values in the PYTHIA generator. The χ^2 corresponds to the MC with the best-fit value of $\sin^2 \theta_W^p$. The uncertainties are statistical only.

$Z/\gamma^* \rightarrow \tau\tau$, diboson (WW and WZ), and $t\bar{t}$ background is $0.20\% \pm 0.05\%$, where the uncertainty is mainly from cross sections of the physics backgrounds.

The effective weak mixing angle is extracted from the background-subtracted A_{FB} spectrum by comparing the data to simulated A_{FB} templates corresponding to different input values of the weak mixing angle. The effective weak mixing angle parameter, here denoted as $\sin^2 \theta_W^p$, corresponds to the input parameter in the calculation from the leading-order PYTHIA generator. Higher-order corrections are used to convert $\sin^2 \theta_W^p$ to $\sin^2 \theta_{\text{eff}}^p$ [21]. The templates are obtained by reweighting the two-dimensional distribution of the Z -boson mass and $\cos \theta^*$ at the generator level to different $\sin^2 \theta_W^p$ PYTHIA predictions. The background-subtracted A_{FB} distribution and PYTHIA predictions are shown in Fig. 1.

The uncertainties on the fitted $\sin^2 \theta_W^p$, listed in Table I, are dominated by the limited size of the data sample. The systematic uncertainties due to muon momentum

TABLE I. Measured $\sin^2 \theta_W^p$ value and corresponding uncertainties. All uncertainties are symmetric. Higher-order corrections are not included.

$\sin^2 \theta_W^p$	0.229 94
Statistical uncertainty	0.000 59
Systematic	
Momentum calibration	0.000 02
Momentum smearing	0.000 04
Background	0.000 03
Efficiencies	0.000 01
Total systematic	0.000 05
PDF	0.000 24
Total	0.000 64

calibration and resolution smearing, the estimation of the backgrounds, and the efficiency scale factors are themselves also dominated by the limited data samples. The PDF uncertainty is obtained as the standard deviation of the distribution of $\sin^2 \theta_W^p$ values given by each of the equal-weighted PDF sets from NNPDF3.0 [15]. The best fit is

$$\sin^2 \theta_W^p = 0.229\,94 \pm 0.000\,59(\text{stat}) \pm 0.000\,05(\text{syst}) \\ \pm 0.000\,24(\text{PDF}).$$

The PYTHIA generator assumes that the effective couplings of leptons, u quarks, and d quarks are the same [5], and it also ignores the mass-scale dependence and complex-valued calculations of the weak corrections and fermion-loop correction to the photon propagator [21]. To correct for these assumptions and reach the common framework used in other measurements [21,22], we shift the value of $\sin^2 \theta_{\text{eff}}^{\ell}$ by $+0.000\,22$ and introduce an additional systematic uncertainty of $0.000\,04$ [21] to get $\sin^2 \theta_{\text{eff}}^{\ell}[\mu\mu] = 0.230\,16 \pm 0.000\,64$.

The D0 e^+e^- measurement [5] and the $\mu^+\mu^-$ measurement presented here are used as inputs to a D0 combination result for $\sin^2 \theta_{\text{eff}}^{\ell}$. The e^+e^- measurement in Ref. [5] has been modified for consistency to incorporate the use of additional higher-order corrections and the NNPDF3.0 PDFs employed in this Letter and in the CDF measurement [4]. The corrected value is $\sin^2 \theta_{\text{eff}}^{\ell}[ee] = 0.231\,37 \pm 0.000\,47$ [21]. The D0 e^+e^- and $\mu^+\mu^-$ measurements agree to within 1.4 standard deviations.

The central values and systematic uncertainties of the e^+e^- and $\mu^+\mu^-$ channels are combined using the inverse of the squares of the statistical uncertainties as weights. The systematic uncertainties are treated as uncorrelated, except the higher-order correction uncertainty which is treated as 100% correlated. However, the total combined uncertainty in practice does not depend on whether the systematic uncertainties of the input measurements are taken to be correlated or uncorrelated, because both measurements are dominated by statistical uncertainties. The correlation of the acceptances between the e^+e^- and $\mu^+\mu^-$ channels cannot be ignored in treating the PDF uncertainty. Instead of estimating a correlation matrix between $\sin^2 \theta_{\text{eff}}^{\ell}$ results for these two channels, a combined PDF uncertainty is estimated by first estimating the PDF uncertainty on the average of values for the e^+e^- and $\mu^+\mu^-$ channels, and then scaling that uncertainty using the linear relation between A_{FB} and $\sin^2 \theta_W^p$ calculated using MC simulations.

The combination is

$$\sin^2 \theta_{\text{eff}}^{\ell}[\text{comb}] = 0.230\,95 \pm 0.000\,35(\text{stat}) \\ \pm 0.000\,07(\text{syst}) \pm 0.000\,19(\text{PDF}).$$

Table II summarizes the inputs and the results of the combination of the e^+e^- and $\mu^+\mu^-$ measurements. The

TABLE II. Combined measurement of $\sin^2 \theta_{\text{eff}}^{\ell}$ and breakdown of its uncertainties, together with the corresponding input values. All uncertainties are symmetric.

	e^+e^- channel	$\mu^+\mu^-$ channel	Combined
$\sin^2 \theta_{\text{eff}}^{\ell}$	0.231 37	0.230 16	0.230 95
Statistical	0.000 43	0.000 59	0.000 35
Systematic	0.000 09	0.000 06	0.000 07
PDF	0.000 17	0.000 24	0.000 19
Total	0.000 47	0.000 64	0.000 40

measured $\sin^2 \theta_{\text{eff}}^{\ell}$ values from D0 and other experiments are compared to the LEP and SLD average in Fig. 2. The D0 combination has an uncertainty close to the precision of the world's best measurements performed by the LEP and SLD Collaborations.

The measured values of the effective weak mixing angle and the mass of the W boson, M_W [23], are complementary in the SM global fit and have different sensitivities to new physics scenarios. As an indicative measure of relative precision, we convert $\sin^2 \theta_{\text{eff}}^{\ell}$ into the W -boson mass using the relationship, valid in the framework of the SM and the on-shell renormalization scheme,

$$\sin^2 \theta_{\text{eff}}^{\ell} = \text{Re}[\kappa_e(M_Z^2)] \times \left(1 - \frac{M_W^2}{M_Z^2}\right),$$

where $\text{Re}[\kappa_e(M_Z^2)]$ is a radiative correction calculated using ZFITTER [22]. The calculated value of $\text{Re}[\kappa_e(M_Z^2)]$ is 1.0371 [24]. The main uncertainty on this quantity is due

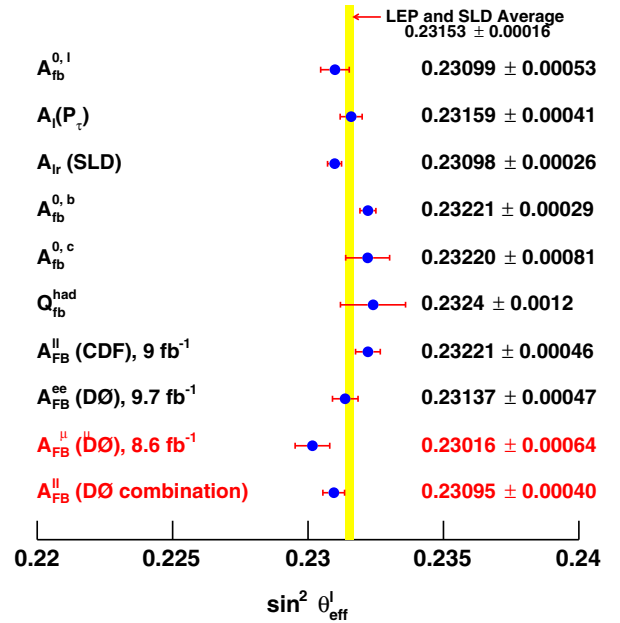


FIG. 2. Comparison of $\sin^2 \theta_{\text{eff}}^{\ell}(M_Z)$ measured by D0 with results from other experiments. The average of measurements from the LEP and SLD Collaborations [1] is also shown.

to the experimental measurement of the top-quark mass $173.2 \pm 0.9 \text{ GeV}/c^2$ [25]. This translates into an uncertainty of 0.000 08 on the value of $\sin^2 \theta_{\text{eff}}^e$. The values of other input parameters, including the electromagnetic fine-structure constant α_{em} with a “running” correction from light-quark contributions, the strong-interaction coupling at the Z-boson mass $\alpha_s(M_Z^2)$, the Fermi constant G_F , and the masses of the Z boson M_Z and the Higgs boson m_H , give uncertainties that are negligible compared to the uncertainty arising from the top-quark mass, as discussed in Ref. [21]. By this procedure, we obtain $M_W = 80\,396 \pm 21 \text{ MeV}/c^2$, with an uncertainty similar to the best direct determination of M_W .

In conclusion, we have measured the effective weak mixing angle parameter from the forward-backward charge asymmetry A_{FB} distribution in the process $p\bar{p} \rightarrow Z/\gamma^* \rightarrow \mu^+\mu^-$ at the Fermilab Tevatron Collider. The primary systematic uncertainty arising from muon momentum calibration is reduced by introducing a charge- η -solenoid-dependent calibration. The final result using 8.6 fb^{-1} of D0 run II data is $\sin^2 \theta_{\text{eff}}^e[\mu\mu] = 0.230\,16 \pm 0.000\,64$, which is at the level of the best single-channel precision from hadron collider experiments. The D0 combination of the e^+e^- and $\mu^+\mu^-$ measurements is $\sin^2 \theta_{\text{eff}}^e[\text{comb}] = 0.230\,95 \pm 0.000\,40$, which is the most precise single-experiment measurement at hadron colliders and is the most precise result based on the coupling of light quarks to the Z boson.

This document was prepared by the D0 Collaboration using the resources of the Fermi National Accelerator Laboratory (Fermilab), a U.S. Department of Energy, Office of Science, HEP User Facility. Fermilab is managed by Fermi Research Alliance, LLC (FRA), acting under Contract No. DE-AC02-07CH11359. We thank the staffs at Fermilab and collaborating institutions, and acknowledge support from the Department of Energy and the National Science Foundation (USA); the Alternative Energies and Atomic Energy Commission and National Center for Scientific Research/National Institute of Nuclear and Particle Physics (France); the Ministry of Education and Science of the Russian Federation, the National Research Center “Kurchatov Institute” of the Russian Federation, and the Russian Foundation for Basic Research (Russia); the National Council for the Development of Science and Technology and the Carlos Chagas Filho Foundation for the Support of Research in the State of Rio de Janeiro (Brazil); the Department of Atomic Energy and the Department of Science and Technology (India); the Administrative Department of Science, Technology and Innovation (Colombia); the National Council of Science and Technology (Mexico); the National Research Foundation of Korea (Korea); the Foundation for Fundamental Research on Matter (Netherlands); the Science and Technology Facilities Council and The

Royal Society (United Kingdom); the Ministry of Education, Youth and Sports (Czech Republic); Bundesministerium für Bildung und Forschung (Federal Ministry of Education and Research) and Deutsche Forschungsgemeinschaft (German Research Foundation) (Germany); Science Foundation Ireland (Ireland); the Swedish Research Council (Sweden); the China Academy of Sciences and the National Natural Science Foundation of China (China); and the Ministry of Education and Science of Ukraine (Ukraine). We thank Willis Sakumoto for his help in assuring that the CDF and D0 Collaborations use a similar phenomenological framework for the $\sin^2 \theta_{\text{eff}}^e$ measurements. We thank Michael Peskin and one of the referees for useful discussions on the relationship between the measured weak mixing angle and the W-boson mass.

*Deceased.

^aVisitor from Augustana College, Sioux Falls, South Dakota 57197, USA.

^bVisitor from Kiev Institute for Nuclear Research (KINR), Kyiv 03680, Ukraine.

^cVisitor from The University of Liverpool, Liverpool L69 3BX, United Kingdom.

^dVisitor from American Association for the Advancement of Science, Washington, D.C. 20005, USA.

^eVisitor from Deutsches Elektronen-Synchrotron (DESY), Notkestrasse 85, Germany.

^fVisitor from P. N. Lebedev Physical Institute of the Russian Academy of Sciences, 119991, Moscow, Russia.

^gVisitor from CONACyT, M-03940 Mexico City, Mexico.

^hVisitor from University College London, London WC1E 6BT, United Kingdom.

ⁱVisitor from Purdue University, West Lafayette, Indiana 47907, USA.

^jVisitor from Centro de Investigacion en Computacion—IPN, CP 07738 Mexico City, Mexico.

^kVisitor from Karlsruher Institut für Technologie (KIT)—Steinbuch Centre for Computing (SCC), D-76128 Karlsruhe, Germany.

^lVisitor from SLAC, Menlo Park, California 94025, USA.

^mVisitor from Office of Science, U.S. Department of Energy, Washington, D.C. 20585, USA.

ⁿVisitor from Universidade Estadual Paulista, São Paulo, SP 01140, Brazil.

^oVisitor from European Organization for Nuclear Research (CERN), CH-1211 Geneva, Switzerland.

^pVisitor from Institute of Physics, Belgrade, Belgrade, Serbia.

^qVisitor from University of Maryland, College Park, Maryland 20742, USA.

- [1] G. Abbiendi *et al.* (LEP Collaborations ALEPH, DELPHI, L3, and OPAL; SLD Collaboration, LEP Electroweak Working Group; SLD Electroweak and Heavy Flavor Groups), Precision electroweak measurement on the Z resonance, *Phys. Rep.* **427**, 257 (2006).

- [2] J. C. Collins and D. E. Soper, Angular distribution of dileptons in high-energy hadron collisions, *Phys. Rev. D* **16**, 2219 (1977).
- [3] T. Aaltonen *et al.* (CDF Collaboration), Indirect measurement of $\sin^2 \theta_W$ or M_W using $\mu^+\mu^-$ pairs from γ^*/Z bosons produced in $p\bar{p}$ collisions at a center-of-momentum energy of 1.96 TeV, *Phys. Rev. D* **89**, 072005 (2014).
- [4] T. Aaltonen *et al.* (CDF Collaboration), Measurement of $\sin^2 \theta_{\text{eff}}^{\text{lept}}$ using e^+e^- pairs from γ^*/Z bosons produced in $p\bar{p}$ collisions at a center-of-momentum energy of 1.96 TeV, *Phys. Rev. D* **93**, 112016 (2016).
- [5] V. M. Abazov *et al.* (D0 Collaboration), Measurement of the Effective Weak Mixing Angle in $p\bar{p} \rightarrow Z/\gamma^* \rightarrow e^+e^-$ Events, *Phys. Rev. Lett.* **115**, 041801 (2015).
- [6] G. Aad *et al.* (ATLAS Collaboration), Measurement of the forward-backward asymmetry of electron and muon pair-production in pp collisions at $\sqrt{s} = 7$ TeV with the ATLAS detector, *J. High Energy Phys.* **09** (2015) 049.
- [7] S. Chatrchyan *et al.* (CMS Collaboration), Measurement of the weak mixing angle with the Drell-Yan process in proton-proton collisions at the LHC, *Phys. Rev. D* **84**, 112002 (2011).
- [8] R. Aaij *et al.* (LHCb Collaboration), Measurement of the forward-backward asymmetry in $Z/\gamma^* \rightarrow \mu^+\mu^-$ decays and determination of the effective weak mixing angle, *J. High Energy Phys.* **11** (2015) 190.
- [9] V. M. Abazov *et al.* (D0 Collaboration), The upgraded D0 detector, *Nucl. Instrum. Methods Phys. Res., Sect. A* **565**, 463 (2006).
- [10] M. Abolins *et al.* (D0 Collaboration), Design and implementation of the new D0 level-1 calorimeter trigger, *Nucl. Instrum. Methods Phys. Res., Sect. A* **584**, 75 (2008).
- [11] R. Angstadt *et al.* (D0 Collaboration), The layer-0 inner silicon detector of the D0 experiment, *Nucl. Instrum. Methods Phys. Res., Sect. A* **622**, 298 (2010).
- [12] D0 uses a cylindrical coordinate system with the z axis along the beam axis in the proton direction. Angles θ and ϕ are the polar and azimuthal angles, respectively. Pseudorapidity is defined as $\eta = -\ln[\tan(\theta/2)]$, where θ is measured with respect to the interaction vertex. In the massless limit, η is equivalent to the rapidity $y = (1/2) \ln[(E + p_z)/(E - p_z)]$, and η_{det} is the pseudorapidity measured with respect to the center of the detector.
- [13] V. M. Abazov *et al.* (D0 Collaboration), Muon reconstruction and identification with the run II D0 detector, *Nucl. Instrum. Methods Phys. Res., Sect. A* **737**, 281 (2014).
- [14] T. Sjöstrand, P. Edén, C. Feriberg, L. Lönnblad, G. Miu, S. Mrenna, and E. Norrbin, High-energy-physics event generation with PYTHIA 6.1, *Comput. Phys. Commun.* **135**, 238 (2001). PYTHIA version v6.323 is used throughout.
- [15] Richard D. Ball *et al.* (NNPDF Collaboration), Parton distributions for the LHC run II, *J. High Energy Phys.* **04** (2015) 040.
- [16] R. Brun and F. Carminati, GEANT detector description and simulation tool, CERN Program Library Long Writup W5013, 1993 (unpublished).
- [17] A. Bodek, A. van Dyne, J.-Y. Han, W. Sakumoto, and A. Srelnikov, Extracting muon momentum scale corrections for hadron collider experiments, *Eur. Phys. J. C* **72**, 2194 (2012).
- [18] C. Balazs and C. P. Yuan, Soft gluon effects on lepton pairs at hadron colliders, *Phys. Rev. D* **56**, 5558 (1997).
- [19] R. Hamberg, W. L. van Neerven, and T. Matsuura, A complete calculation of the order- α_s^2 correction to the Drell-Yan k -factor, *Nucl. Phys.* **B359**, 343 (1991); Erratum, *Nucl. Phys.* **B644**, 430 (2002).
- [20] M. L. Mangano, F. Piccinini, A. D. Polosa, M. Moretti, and R. Pittau, ALPGEN, a generator for hard multiparton process in hadronic collisions, *J. High Energy Phys.* **07** (2003) 001.
- [21] T. Aaltonen *et al.* (CDF and D0 Collaborations), Tevatron run II combination of the effective leptonic electroweak mixing angle, [arXiv:1801.06283](https://arxiv.org/abs/1801.06283).
- [22] Arif Akhundov, Andrej Arbuzov, Sabine Riemann, and Tord Riemann, ZFITTER 1985–2013, *Phys. Part. Nucl.* **45**, 529 (2014).
- [23] T. Aaltonen *et al.* (CDF and D0 Collaborations), Combination of CDF and D0 W -boson mass measurements, *Phys. Rev. D* **88**, 052018 (2013).
- [24] T. Aaltonen *et al.* (CDF Collaboration), Indirect measurement of $\sin^2 \theta_W(M_W)$ using e^+e^- pairs in the Z -boson region with $p\bar{p}$ collisions at a center-of-momentum energy of 1.96 TeV, *Phys. Rev. D* **88**, 072002 (2013); Erratum, *Phys. Rev. D* **88**, 079905 (2013).
- [25] T. Aaltonen *et al.* (CDF and D0 Collaborations), Combination of the top-quark mass measurements from the Tevatron collider, *Phys. Rev. D* **86**, 092003 (2012).